



# Pseudodynamic testing of a full-size two-story reinforced concrete frame retrofitted with an H-section steel frame installed using a length-adjustment control box

Ju-Seong Jung<sup>1</sup> · Kang-Seok Lee<sup>1</sup>

Received: 21 December 2019 / Accepted: 8 June 2020 / Published online: 12 June 2020  
© Springer Nature B.V. 2020

## Abstract

In this study, to overcome the construction drawbacks of conventional seismic retrofitting techniques, we proposed a new H-section steel frame (HSF) system for seismic strengthening of existing medium-to-low-rise reinforced concrete (RC) buildings. This HSF strengthening method exhibits excellent constructability because a control box is applied as a length adjustment device to cope with errors in the field associated with assembly works between the existing structure and reinforcing frame. The method represents a strength design approach implemented via retrofitting, to easily increase the ultimate lateral load capacity of RC buildings lacking seismic data, which exhibit shear failure. Two full-size two-story RC frame specimens were designed based on an existing RC building in Korea lacking seismic data, and then strengthened using the HSF system; thus, one control specimen and one specimen strengthened with the HSF system were used. Pseudodynamic tests were conducted to verify the effects of seismic retrofitting, and the earthquake response behavior with use of the proposed method, in terms of the maximum response strength, response displacement, and degree of earthquake damage compared with a control RC frame. Nonlinear dynamic analysis was performed based on the material properties of the test specimens, including a mathematical nonlinear hysteresis model to compare the results of the pseudodynamic tests. Test results revealed that the proposed HSF strengthening method, internally applied to the RC frame, effectively increased the lateral ultimate strength, resulting in reduced response displacement of RC structures under large-scale earthquake conditions. The nonlinear dynamic analysis and test results were in good agreement.

**Keywords** Non-linear dynamic analysis · Pseudodynamic · Reinforced concrete · Seismic capacity · Seismic strengthening

---

✉ Kang-Seok Lee  
ksleenist@hanyang.ac.kr

<sup>1</sup> Department of Architectural Engineering, Hanyang University, Ansan, Republic of Korea

## 1 Introduction

Many existing buildings have excellent durability and can be used semi-permanently if appropriate designs, materials, and construction techniques are applied. However, buildings may be subjected to artificial and physical damage due to natural disasters after construction, and various defects occur over time due to aging, including chemical and physical deformation. Earthquakes are among the most hazardous natural disasters, and the destruction of building structures vividly demonstrates the severity of earthquake damage, as observed during a recent series of earthquakes.

Long-term earthquake observation and research has improved our understanding of their behaviors, including patterns of damage to building structures, and significant efforts have been made to mitigate earthquake damage to new buildings through seismic design. Correlations between the degree of damage caused by earthquakes and the seismic resistance mechanisms of structures have been subjected to vigorous theoretical and experimental investigations. Procedures for calculating shear forces and dynamic responses based on the results of these studies have been adopted in seismic design codes and standards during recent decades, including the International Building Code (IBC 2018), Building Code Requirements for Structural Concrete of the American Concrete Institute (ACI 318-14 2014), Standard for Structural Calculation of Reinforced Concrete Structures of the Architectural Institute of Japan (AIJ 2010), and the Korean Building Code (KBC 2016). Progress in seismic design has resulted in new buildings with improved prospects for satisfactory behavior during earthquakes.

Innovations in seismic design methodologies have led designers to question the adequacy of the seismic behavior of existing buildings lacking seismic data, including those affected by the 2008 Sichuan earthquake in China, the 2010 Chile earthquake, the 2011 Christchurch earthquake in New Zealand, the 2012 Great East Japan earthquake, the 2013 Lushan earthquake in China, the 2016 Kumamoto earthquake in Japan, the 2017 Pohang earthquake in South Korea, and the 2018 Hokkaido Eastern Iburi earthquake. According to the results of previous investigations of earthquake damage, including those listed above, a large proportion of earthquake damage occurs in medium-to-low-rise buildings with fewer than six stories, especially reinforced concrete (RC) buildings lacking seismic data. Therefore, it is necessary to retrofit existing medium-to-low-rise RC buildings lacking seismic data to be resistant against earthquakes, and important existing buildings are required to be fully operational even under severe earthquake conditions.

Over the past three decades, rehabilitation procedures for existing RC buildings have been promoted, leading to the development of several seismic strengthening techniques to improve their seismic performance. These methods include techniques to improve ultimate strength or deformation capability (Abou-Elfath and Ghobarah 2000; Ariyaratana and Fahnstock 2011; Badoux and Jirsa 1990; Celik and Bruneau 2009; Ghobarah and Abou-Elfath 2001; Lee 2015; Maheri et al. 2003; Ju et al. 2014; Nateghi-Alahi 1995; Onat et al. 2018; Sarno and Elnashai 2009; Smith and Kim 2008; Sugano 1981; Witt 2007), as well as technology for vibration control (Hwang and Lee 2016; Kunisue et al. 2000; Marko et al. 2004; Suzuki et al. 1998) and seismic isolation (Oliveto et al. 2004). Most medium-to-low-rise RC buildings lacking seismic data feature column hoop spacing of approximately 30 cm or wider, resulting in a high risk of shear failure. For these RC buildings, retrofitting methods that adopt independent construction techniques for improving ductility have been shown to be inefficient due to extremely inadequate ultimate horizontal strength. Retrofitting techniques that increase strength to improve the seismic performance of medium-to-low-rise

RC buildings lacking seismic data are more efficient when there is a high risk of shear failure (AIJ 1968; Maeda et al. 2004; Lee et al. 1995; Lee 2010; FEMA 310 1998; FEMA 356 2000; JBDPA 2005, 2017).

Among existing methods for seismic strengthening, the most popular are the addition of infill shear walls within the frame, installation of steel braces, such as K and X braces, within the frame, insertion of steel plate panel walls into the frame, and section enlargement. These seismic strengthening methods are effective for improving building strength to resist horizontal forces (FEMA 356 2000; JBDPA 2017). However, these conventional methods increase building weight; buildings with weak foundations, such as RC buildings with non-seismic details, may require foundation reinforcement due to the weight increase. Precise construction is also required to connect post-installed anchor systems between existing frame structures and strengthening members. It is highly likely that the seismic strengthening construction period will be extended due to the need to fabricate strengthening members after on-site measurements, or because wet methods using non-shrink mortar or other such materials are applied (SSRG 2008; Lee et al. 2009; Lee and Shin 2013).

To overcome these drawbacks of conventional seismic retrofitting for increased ultimate strength, it is essential to develop a new retrofitting construction method suited to the seismic structural characteristics of medium-to-low-rise RC buildings with non-seismic details, considering shear failure type, a weak foundation, and low lateral-ultimate strength. Any such new technology should ensure integrity between the existing structure and seismic reinforcement device.

In this study, a new H-section steel frame (HSF) system was proposed for seismic strengthening of existing medium-to-low-rise RC buildings to overcome the drawbacks of drawbacks of the conventional seismic retrofitting techniques. The HSF strengthening method developed in this study exhibits excellent constructability because a control box is applied as a length adjustment device to cope with errors associated with assembly works between the existing structure and reinforcing frame in the field. The method represents a strength design approach implemented via retrofitting, to easily increase the ultimate lateral load capacity of RC buildings lacking seismic data, which have shear failure mode. Figure 1 shows a post-construction image of the proposed HSF system.

Test specimens strengthened with the HSF system were designed on the basis of typical existing RC buildings constructed prior to the seismic code revision in Korea. Two full-size two-story RC frame specimens were fabricated: one specimen strengthened with the HSF system and one control specimen. Pseudodynamic tests were conducted to verify the effects of seismic retrofitting, according to earthquake levels specified by the KBC (2016). The earthquake response behavior of the proposed method, in terms of maximum response strength, response displacement, and the degree of earthquake damage was compared with that of the control RC frame. We also performed a nonlinear dynamic analysis based on the material properties of the test specimens using a mathematical nonlinear hysteresis model, and compared the results to those of the pseudodynamic tests.

## 2 Overview of the HSF strengthening method

When applying conventional seismic strengthening methods, which connect the existing RC frame and steel frame strengthening element, additional time is required for construction because the reinforcing steel frame is produced after on-site measurements. If the steel frame is produced in advance, it is difficult to achieve precise joint construction due to



Fig. 1 Post-construction image of the H-section steel frame (HSF) strengthening system

errors associated with assembly works aimed at connecting the existing frame and the steel frame strengthening elements. Indirect connection methods using non-shrink mortar are applied to compensate for this problem; however, cracks in the joints are inevitable in the event of an earthquake. The occurrence of cracks attenuates the transfer of seismic loads to the seismic reinforcement device, thus reducing the seismic reinforcement effect expected to arise through the integrated behavior of the existing structure and the seismic reinforcement device.

The proposed HSF strengthening method (Fig. 2), uses a control box installed as a length adjustment device to cope with errors in the field associated with assembly works

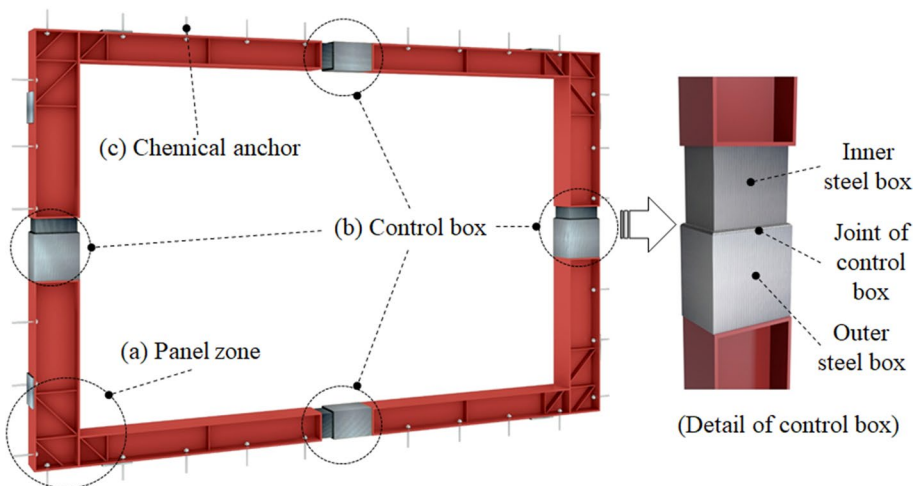
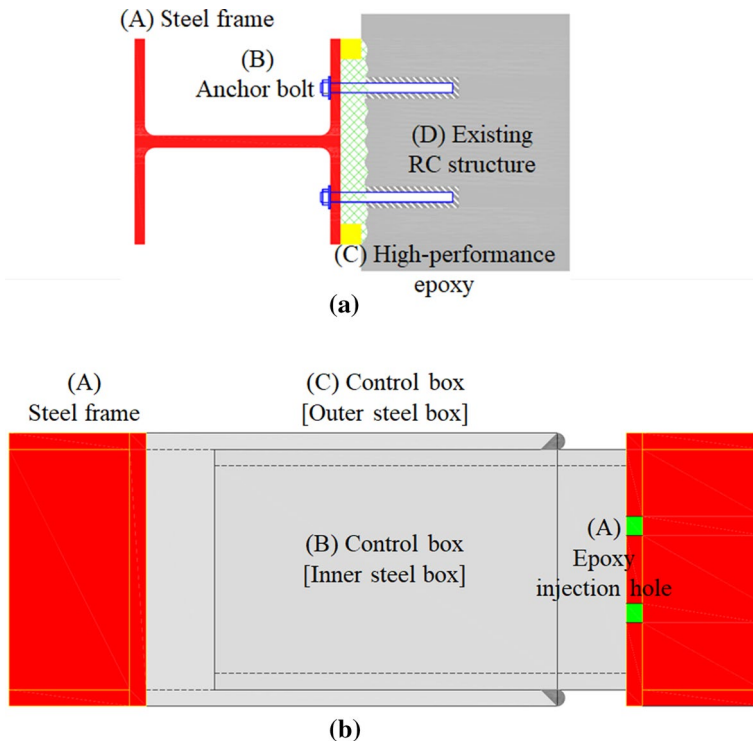


Fig. 2 Detailed diagram of the HSF strengthening system

aimed at connecting the existing structure and the reinforcing steel frame. The control box can be adjusted within a range of 250 mm using the piston structure, resulting in a direct connection method. Thus, the HSF system proposed in this study effectively enhances seismic performance by improving the ultimate lateral load capacity of existing medium-to-low-rise RC buildings lacking seismic data.

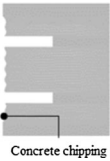
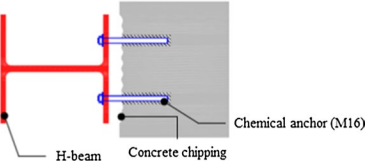
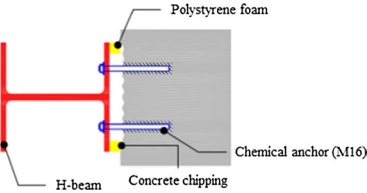
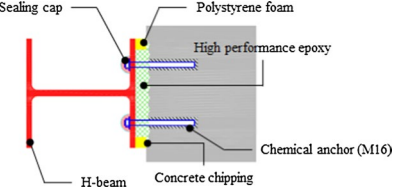
Figure 3a shows details of the connection elements of the HSF retrofitting system; details of the control box are shown in Fig. 3b. As shown in Fig. 3a, the HSF connection method consists of (A) a steel frame for seismic strengthening, (B) an anchor bolt for jointing, (C) a high-performance epoxy, and (D) an existing RC structure. A major feature of the HSF connection system is that the steel frame for reinforcement (A) and the existing RC structure (D) are completely jointed by the anchor bolt (B) and fixed by the high-performance epoxy (C). This connection results in integration of the existing RC structure with the reinforcing member. Table 1 lists the construction steps for the method. The steel material of the strengthening member is SS400.

The control box shown in Fig. 3b consists of a steel frame for seismic strengthening (A), an inner steel box (B), an outer steel box (C), and an epoxy injection hole (D). The control box copes with assembly works errors that may occur in the field, and piston structural behavior between the inner and outer steel boxes allows length adjustment within a range of 250 mm. After length adjustments have been completed, the cross-section of the control box is bonded by welding and epoxy injection.



**Fig. 3** Detailed diagram of a connection element and technical details of the HSF strengthening system. (a) Connection method. (b) Control box

**Table 1** Construction procedure for the H-section steel frame (HSF) strengthening system

Sequence	Construction procedure
1  Concrete chipping	Boring of anchoring hole and chipping of concrete surface
2  H-beam Concrete chipping Chemical anchor (M16)	Installation of anchor and steel frame for strengthening
3  Polystyrene foam H-beam Concrete chipping Chemical anchor (M16)	Installation of polystyrene foam
4  Sealing cap Polystyrene foam High performance epoxy H-beam Concrete chipping Chemical anchor (M16)	Sealing of high-performance epoxy, and finishing by mortar

### 3 Test specimens

#### 3.1 Specimen design and variables

To verify the seismic strengthening effectiveness of the HSF system, we selected the frame of a typical three-story Korean RC building with non-seismic details (Lee and Shin 2013) designed in the 1980s. Figure 4 shows front and planar views of the investigated RC building and a frame selected for the pseudodynamic test. The specified compressive strength of the concrete used in this building was 21 MPa, and the story height was 3300 mm. The structure consisted of a pure RC frame with spandrel walls in the longitudinal direction, and in-filled brick walls in the transverse direction.

The test target (Fig. 4) was a one-span two-story full-size frame on the inner side (X2-3) of the exterior frame (Y3) in the longitudinal direction, including columns and beams. This building type was selected for testing because the seismic capacity of in-filled brick walls in the transverse direction is higher than that in the longitudinal direction (FEMA 356 2000; JBDPA 2005). The configurations of the full-size specimens are shown in Figs. 5 and 6. The purpose of the tests was to verify the seismic strengthening effectiveness of the HSF system, in terms of maximum response strength, response

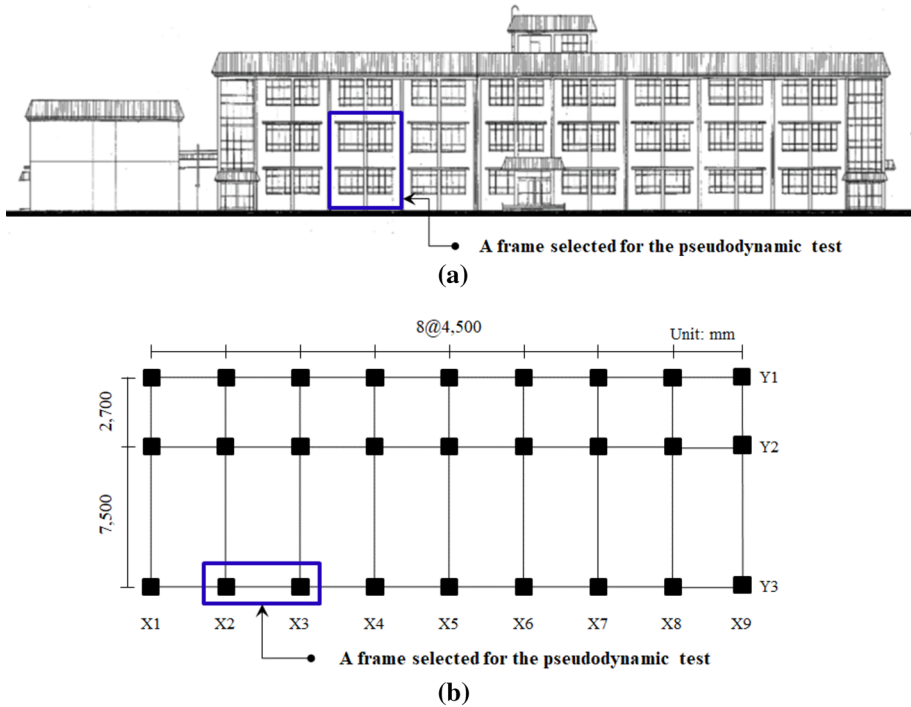


**Fig. 4** Front and planar views of the investigated building and a frame selected for the pseudodynamic test. (a) Front view. (b) Planar view

displacement, degree of earthquake damage, and hysteresis in the lateral load-drift relationship, compared with the control specimen.

Table 2 lists the variables and provides a summary of the specimens tested. A total of three test specimens were prepared: one control test specimen (nonstrengthened, PD-RC) and one test specimen strengthened with the HSF system (PD-HSF) for the pseudodynamic test. All specimens had identical dimensions and rebar arrangements. The column cross-section was 350 mm × 500 mm, and the ratio of column clear height to depth ( $h_0/l$ ) was 6.8. Each column had an 8-D19, 2-D16 SD400 main rebar reinforced with D10 steel shear reinforcement bars at 300-mm intervals. The cross-sectional area of the beam on each floor was 250 mm × 450 mm, and that of the underground beam was 350 mm × 600 mm. All beams were planned as T-type beams, considering the effective width of the slab (KBC 2016).

The ground motion acceleration in the pseudodynamic test was east–west (EW) ground motion, recorded at Hachinohe (Table 2) during the 1968 Tokachi-oki earthquake, which caused severe damage to many medium-to-low-rise RC buildings constructed before the seismic code revision in Japan. The Hachinohe ground motion has been widely used to verify seismic performance in medium-to-low-rise RC building systems.

The magnitude of ground motion was normalized to acceleration values of 2, 3, and 4  $m/s^2$ . The ground motion acceleration of 2 and 3  $m/s^2$  approximately corresponds to the seismic load in Zone-1 with SD- and SE-soil conditions, under which two thirds of the earthquake ground motion has a 2% probability of exceedance within 50 years (i.e., a

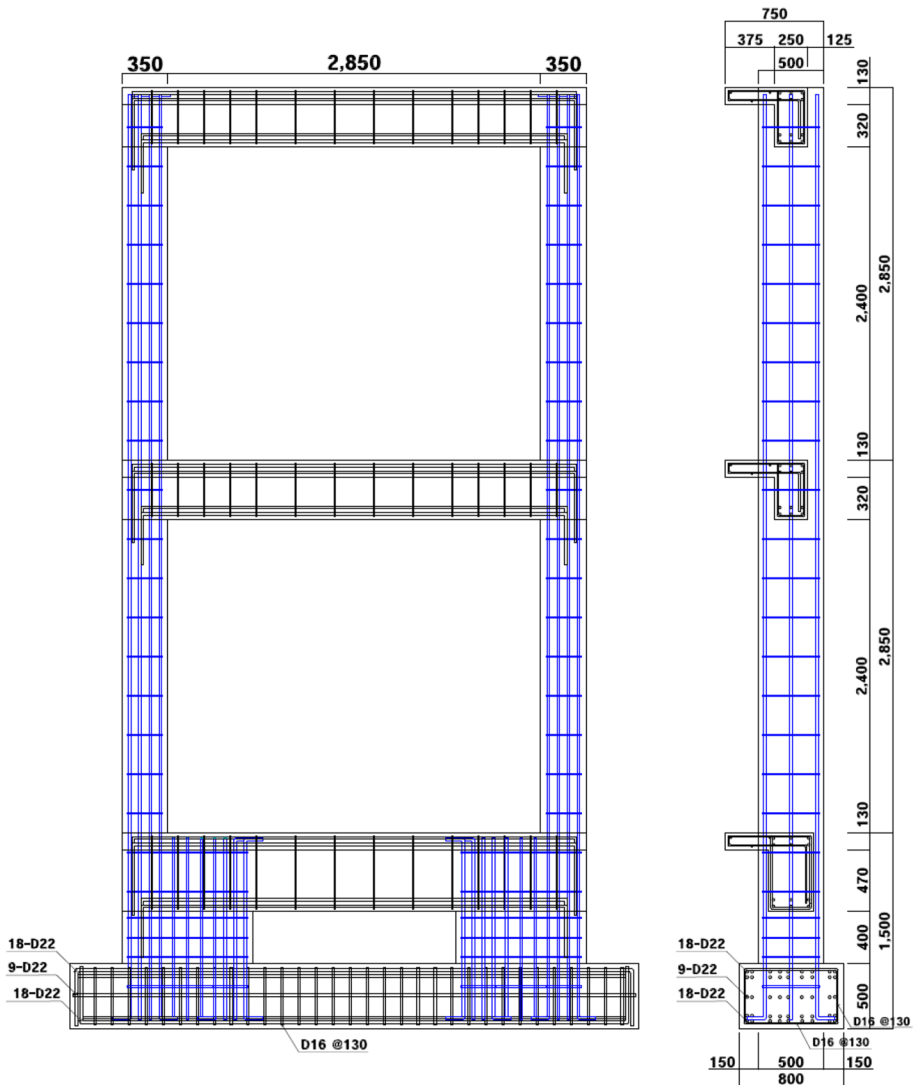


**Fig. 5** Detailed configuration of the control specimen and strain gage locations

2500-year return period), as specified by KBC (2016). Ground motions of  $4 \text{ m/s}^2$  were also used, to assess the seismic strengthening effectiveness of the HSF system in the context of a very strong earthquake, under which all earthquake ground motion has a 2% probability of exceedance within 50 years. The axial load applied to the actual existing frame (two columns), i.e., 1000 kN, was divided equally and an axial force of 500 kN was constantly applied to each column during pseudodynamic testing.



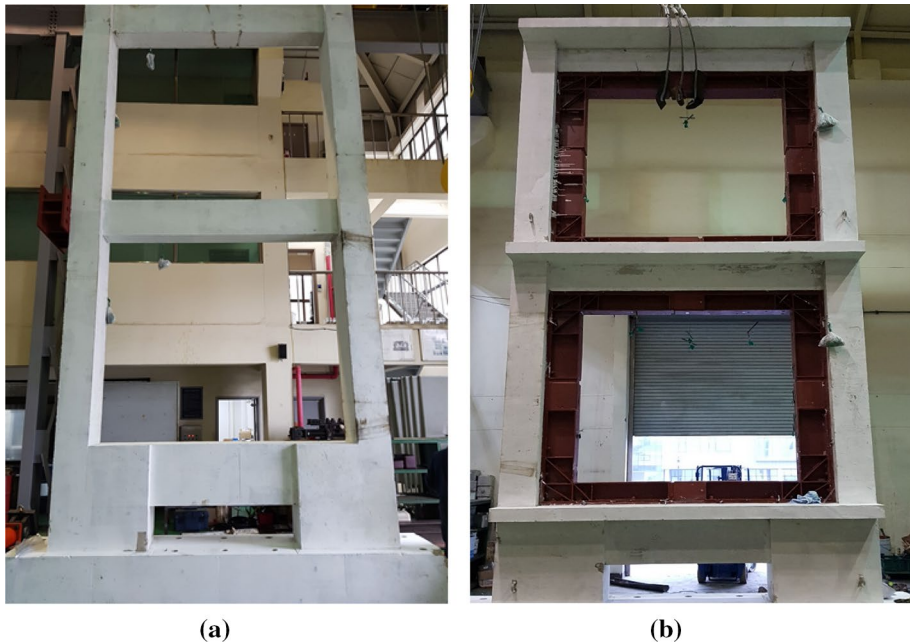


**Fig. 6** Detailed configuration of the test specimen. **(a)** Control specimen. **(b)** HSF-strengthened specimen

**Table 2** Summary of the test conditions for pseudodynamic tests

Specimen	Test method	Strengthening type	Earthquake levels ( $m/s^2$ )
PD-RC	Pseudodynamic	The control specimen	Hachinohe (EW): 2
PD-HSF	Pseudodynamic	The internal HSF connection method	Hachinohe (EW): 2, 3, 4

### 3.2 Material properties

The compressive strength of the concrete for each specimen used in the structural experiment was designed to be 21 MPa. Cylindrical compression tests yielded a value of  $21 \pm 1.13$  MPa. The reinforcing rebar was type 1 SD400. For column members, D19 and D16 were used as the main reinforcements and D10 was used as the hoop reinforcement. To investigate the material properties of the rebar used in the specimens, three rebar tensile test specimens for each of the D19, D16, and D10 reinforcements were fabricated, and tensile tests were conducted at a loading rate of 5 mm/min using a universal testing machine (UTM) in accordance with regulations specified in KS B 0801 (2017). The test results showed average yield strength and tensile strength values of 491 and 731 MPa, respectively, for both D19 and D16, and 477 and 711 MPa for D10.

### 3.3 Joint connection design of the HSF seismic strengthening method

The type, embedding depth, and anchor space of the joint connections for the HSF strengthening system were based on the anchor design provided by the JBDPA (2005). The results of the anchor design for the HSF connection method are listed in Table 3. Figure 6 shows the configuration of a test specimen strengthened using the HSF system, based on the joint connection results shown in Table 3.

The joint connection anchors had a diameter ( $D$ ) of 16 mm and spacing of 200 mm, in double arrangement. A total of 18 and 16 anchors were used in each beam and column, respectively. The strength of the joint connections was approximately 1.7-fold higher for the  $L_B$ , and 1.79-fold higher for the  $L_C$  than the lateral resisting force on the HSF strengthening frame (Table 3). The HSF system proposed in this study was able to resist the seismic load when used with the existing RC frame.

## 4 Pseudodynamic testing procedures

### 4.1 Overview of pseudodynamic testing

The optimal method for evaluating the non-linear response characteristics of a test structure, e.g., a building subjected to earthquake ground motions, is a full-scale structural test performed on a shaking table. Generally, such a test is not possible within current experimental facilities, and will never be practical for most large structures. Several alternative approaches have been developed, including shaking table tests of reduced-scale structural models. The drawbacks of such reduced-scale tests are obvious; many structures cannot be adequately represented by reduced-scale structural models.

The pseudodynamic test method was developed to conduct realistic experimental tests on full-scale structures subjected to earthquake ground motions (Takanashi et al. 1980; Shing et al. 1984; Shing and Mahin 1985; Mahin and Shing 1985). This test uses an online computer and associated test instrumentation to monitor and control a structure, such that displacement thereof closely resembles the consequences of real seismic excitation. The pseudodynamic test is as realistic as shaking table-based testing, where discretization of the model is feasible; its advantages over shaking tables include (a) versatility, where it allows for detailed observation of the specimen during the test, (b) the ability to test full- and large-scale models, thus circumventing the problem of dynamic similitude, (c) lack of requirement for physical structures, because the method uses a numerical model, (d) greatly reduced equipment, installation, and operation costs, (e) circumventing the problems associated with the interactions of a shaking table with heavy specimens, and (f) improved actuator control and data acquisition reliability

**Table 3** Joint connection design of the HSF system

Member	Member length	Number of anchors	$V_f$ (kN)	$\Sigma V_{ac}$ (kN)	Safety ratio
Beam	$L_B$	18	268.8	455.8	1.70
Column	$L_C$	16	226.3	405.1	1.79

$L_B$ : beam length;  $L_C$ : column length;  $V_f$ : lateral resisting force on the HSF strengthening frame;  $\Sigma V_{ac}$ : strength of joint connections using anchors

due to the relatively slow rate of loading. In principle, the test can be performed in real time; however, physical limitations of the instrumentation dictate that the test must be conducted step-by-step, i.e., pseudodynamically. Shaking table tests may be more appropriate in cases where strain rate effects are significant and/or in distributed parameter systems.

Experimental measurements of restoring forces are performed during the test. These measured forces are then fed into the computer, together with a set of mathematical equations for inertial response characteristics, to determine the structural displacement that would occur as a consequence of a given ground acceleration. This procedure is superior to quasi-static testing because non-linear structural characteristics are based on instantaneous experimental feedback rather than hypothetical mathematical models. Pseudodynamic testing differs from classical computer-based structural dynamic simulations, in that the latter depend on experimentally measured restoring forces rather than on restoring forces computed using a mathematical model.

#### 4.2 Description of the pseudodynamic testing system used in this study

A simplified schematic diagram of the pseudodynamic testing system used in this study is shown in Fig. 7, together with the test configuration. The system can be expressed as a two-degree-of-freedom (TDF) structure. During the test, the computed displacement response is imposed on the specimen via two hydraulic actuators that horizontally installed on the reaction wall. The actual restoring forces are physically measured during the test and used by the control computer to calculate the displacement. Data transformation is achieved using an analog-to-digital/digital-to-analog converter (DA-16A; Tokyo Soki Kenkyujo Company 2020). Filtering and amplification are performed to ensure reliable results and accurate closed-loop control.

We used a pseudodynamic testing program (MTS 2002) to calculate displacement based on the equation of motion of the TDF structure, as determined by the control computer:

$$M\ddot{y}(t) + C\dot{y}(t) + r(t) [= Ky(t)] = -M\ddot{u}, \tag{1}$$

where  $M$ ,  $C$ , and  $K$  are the mass, damping, and stiffness matrices of the structure,  $y$  is a vector of the relative displacement of the mass with respect to its base,  $r$  is the hysteresis restoring force vector, and  $\ddot{u}$  is the base acceleration.

The time integration scheme adopted for solving the equation of motion was an adaptive time-stepping algorithm (Shing et al. 1996; Bursi et al. 1994; Bursi and Shing 1998), developed based on the  $\alpha$ -method proposed by Hilber et al. (1977). The algorithm for numerical integration of the pseudodynamic test is expressed as follows:

$$Ma_{i+1} + (1 + \alpha)Cv_{i+1} - \alpha Cv_i + (1 + \alpha)r_{i+1} - \alpha r_i = (1 + \alpha)f_{i+1} - \alpha f_i, \tag{2}$$

with

$$y_{i+1} = y_i + \Delta t v_i + \Delta t^2 \left[ \left( \frac{1}{2} - \beta \right) a_i + \beta a_{i+1} \right] \tag{3}$$

$$v_{i+1} = v_i + \Delta t \left[ (1 - \gamma) a_i + \gamma a_{i+1} \right] \tag{4}$$

where  $y_i$ ,  $v_i$ , and  $a_i$  are vectors of nodal displacements, velocities, and accelerations at the time equal to  $i\Delta t$ , respectively,  $\Delta t$  is the integration time step,  $r_i$  is the nodal restoring

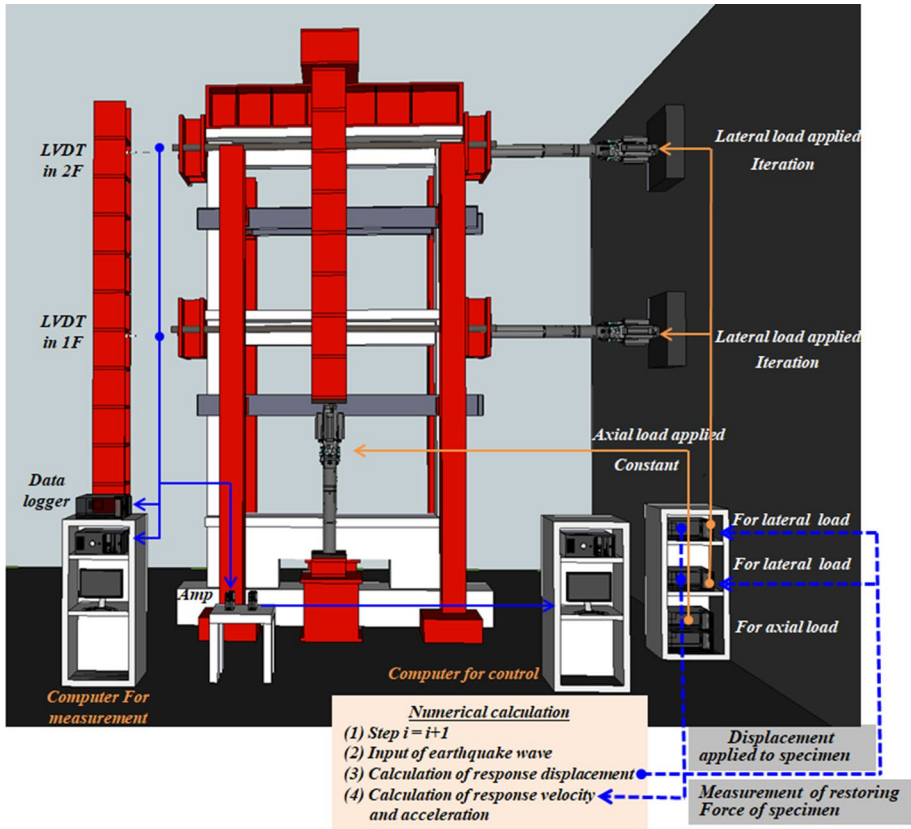
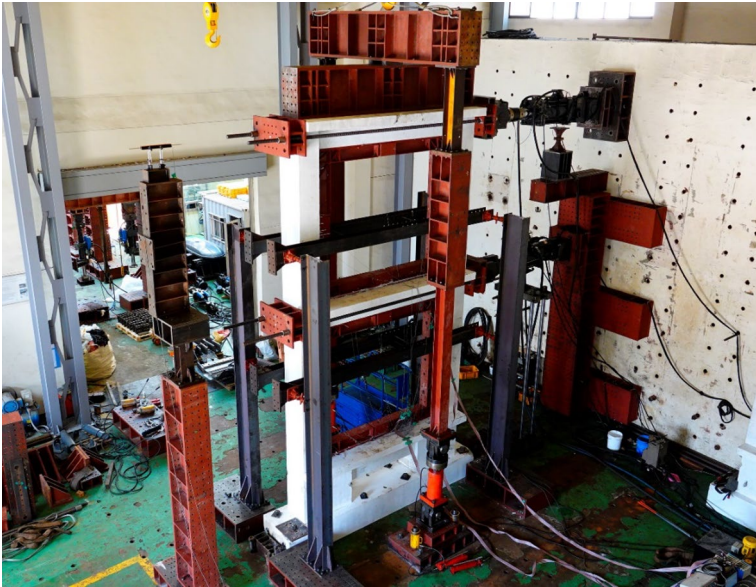


Fig. 7 Simplified schematic diagram of the pseudodynamic testing system used in this study

force vector, and  $f_i$  is the external force excitation vector (i.e.,  $-m\ddot{u}_i$ ). For a linearly elastic structure,  $r_i = Ky_i$  in which  $K$  is the elastic stiffness matrix of the structure.  $\alpha$ ,  $\beta$ , and  $\gamma$  are parameters that govern the numerical properties of the algorithm, which is unconditionally stable when  $-0.5 \leq \alpha \leq 0$ ,  $\beta = \frac{(1-\alpha)^2}{4}$ , and  $\gamma = \frac{1}{2} - \alpha$ .

The displacement response for the next time step was calculated using Eqs. (1)–(4), based on the stiffness ( $K$ ), mass ( $M$ ), and stiffness proportional damping coefficient ( $C$ ), in which the damping ratio was assumed to be 0.03 (i.e., 3% of the critical damping value). Two 2000-kN hydraulic actuators were used to apply the lateral loads, as depicted in Fig. 7. The horizontal displacement used to calculate the displacement response was measured using two 300-mm linear variable differential transformers (LVDTs), installed in each floor. Each column was subjected to a constant vertical load of 500 kN, which is half of the total weight of one-span two-story full-size frame on the inner side (X2-3) of the exterior frame (Y3) in the longitudinal direction, using two 1000-kN oil jacks. The ground motion acceleration for the pseudodynamic test was the EW ground motion recorded at Hachinohe during the 1968 Tokachi-oki earthquake. As stated previously, the magnitude of ground motion was normalized to acceleration



**Fig. 8** Test configuration

values of 2, 3, and 4  $\text{m/s}^2$ , based on the KBC (2016). Figure 8 shows the experimental configuration for the pseudodynamic test.

## 5 Experimental results

Crack and failure characteristics of the control specimen (PD-RC) and the pseudodynamic specimen strengthened by the HSF method (PD-HSF) were investigated. The seismic reinforcement effects of the strengthened specimen (PD-HSF) were compared to the control specimen (PD-RC) by analyzing the lateral load–drift relation curve (restoring force), the time history curve for response displacement, and the maximum seismic response.

### 5.1 Crack and failure patterns

#### (1) Unreinforced control specimen (PD-RC)

A small flexural crack occurred in the PD-RC specimen, at the top and bottom of the columns at 2.34 s with a lateral drift of 18 mm, under input ground motion of 2  $\text{m/s}^2$ . At 2.95 s, with a lateral drift of 45 mm, the flexural cracks extended and shear cracks occurred at the bottoms of the columns. After 3.17 s, the width of the shear cracks that occurred at the bottoms of the columns increased significantly. At 3.3 s, severe concrete spalling began, and at approximately 3.4 s, which showed the maximum response strength of 249 kN and displacement of 66.4 mm, the control specimen exhibited shear failure at the bottom of the first-floor frame (Fig. 9). These results are in agreement with those of a previous study (Lee 2015), indicating that the control specimen, which was designed based on an existing RC school building with non-seismic details, is

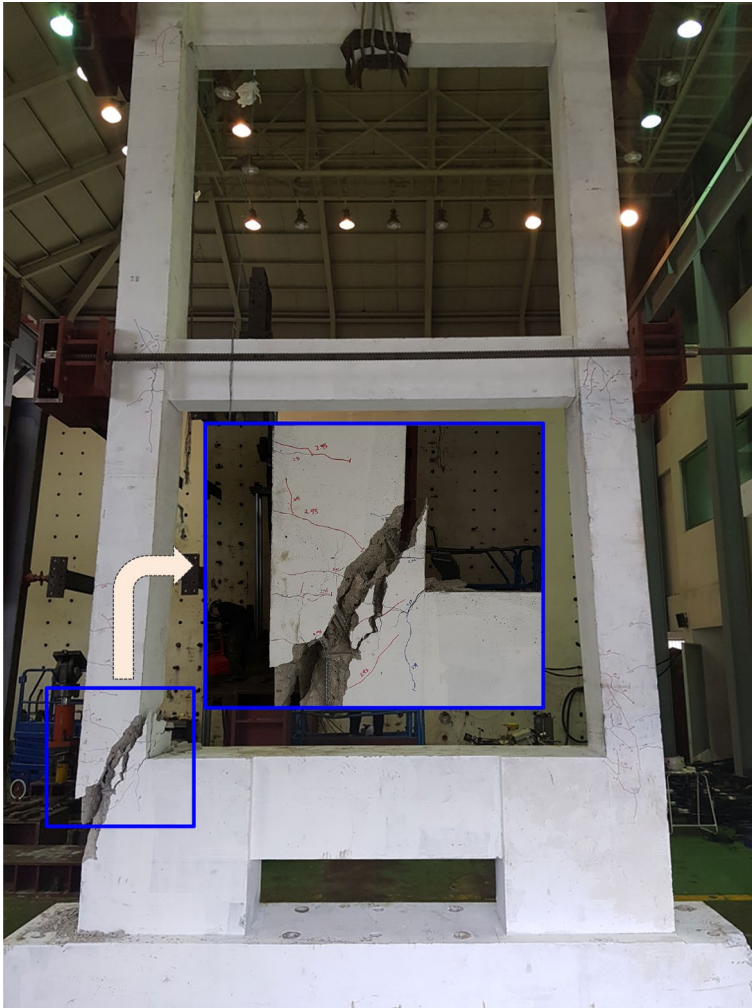


**Fig. 9** Shear failure occurred in the PD-RC specimen during pseudodynamic testing at  $2 \text{ m/s}^2$ , after 3.3 s, with lateral displacement of 66.4 mm

highly vulnerable to seismic damage in the event of a  $2 \text{ m/s}^2$  earthquake. These are important results that demonstrate the necessity of applying seismic reinforcement to school buildings with non-seismic details that were built in the 1980s.

(2) Specimen strengthened with the HSF method (PD-HSF)

Figure 10 shows the crack pattern observed in the PD-HSF specimen during pseudodynamic test, performed by applying earthquake ground motions of 2, 3, and  $4 \text{ m/s}^2$  (Hachinohe, EW). As previously stated, ground motion acceleration rates of 2 and  $3 \text{ m/s}^2$  approximately correspond to the seismic load in Zone-1 under SD and SE soil conditions, which represent two-thirds of the earthquake ground motion, with a 2% probability of exceedance within 50 years, as specified in the KBC (2016). Ground

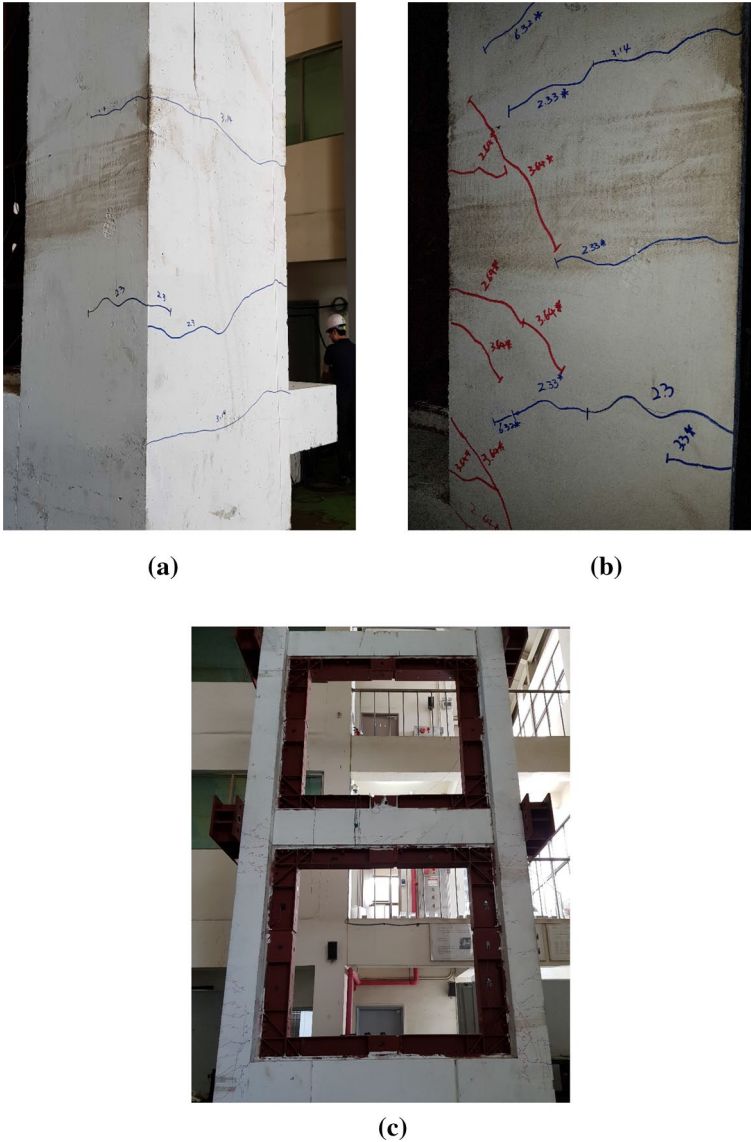


**Fig. 10** Cracks appeared in the PD-HSF specimen during pseudodynamic testing, after (a) 3.14 s with lateral displacement of 10.6 mm at  $2 \text{ m/s}^2$ , (b) 6.32 s with lateral displacement of 24.9 mm at  $3 \text{ m/s}^2$ , and (c) during the final stage at  $4 \text{ m/s}^2$  (10 s)

motion of  $4 \text{ m/s}^2$  was additionally applied to determine the seismic strengthening effectiveness of the HSF system in the context of a very strong earthquake, which represents an earthquake ground motion with a 2% probability of exceedance within 50 years.

In PD-HSF, a specimen strengthened with the developed HSF method, a fine initial flexural crack occurred at the top and bottom of the columns at 2.3 s, with lateral displacement

of 5.84 mm, under  $2 \text{ m/s}^2$  earthquake ground motion. The number of flexural cracks increased after 3.14 s, with lateral drift of 10.6 mm; the degree of cracking was not serious, as shown in Fig. 10a.

However, under input ground motion of  $3 \text{ m/s}^2$ , the number of flexural cracks increased compared to those of  $2 \text{ m/s}^2$  after 2.33 s, with a lateral displacement of 15.3 mm, but the scale was similar to that at  $2 \text{ m/s}^2$ . Shear cracks occurred at approximately 3.64 s, with a lateral drift of 27.2 mm, and increased in number; however, the degree of cracking was not serious, similar to  $2 \text{ m/s}^2$  (Fig. 10b). The reinforced PD-HSF specimen showed light earthquake damage, with a maximum response strength of 656.4 kN and a lateral drift of 33.5 mm at 6.4 s under earthquake ground motion of  $3 \text{ m/s}^2$ . Greater strength was observed in comparison with the nonstrengthened control PD-RC specimen, in which major earthquake damage and shear failure were observed at the bottom of the first-floor frame.

With earthquake ground motion of  $4 \text{ m/s}^2$ , the degree of flexural and shear cracking increased compared to  $3 \text{ m/s}^2$  (Fig. 10b). Wide cracks occurred in the final stage, but these were less than 1.0 mm in length, resulting in less earthquake damage compared to the collapsed PD-RC specimen (Fig. 9). The maximum response strength was 810 kN, with a displacement of 55 mm at 6.4 s. These results validate the HSF strengthening system for earthquakes of 2, 3, and  $4 \text{ m/s}^2$ .

## 5.2 Load–displacement relationships and earthquake damage estimation

Figures 11, 12, and 13 show the lateral response load–displacement relationships (first floor) of the PD-HSF specimen during pseudodynamic testing at 2, 3, and  $4 \text{ m/s}^2$ , respectively, of EW ground motion recorded at Hachinohe during the 1968 Tokachi-oki earthquake. Ground motion acceleration of 2 and  $3 \text{ m/s}^2$  approximately corresponded to the seismic load in Zone-1 with  $S_D$ - and  $S_E$ -soil conditions, under which two thirds of the earthquake ground motion has a 2% probability of exceedance within 50 years. We also used ground motion of  $4 \text{ m/s}^2$  to assess the seismic strengthening effectiveness of the HSF system under very strong earthquake conditions, where all earthquake ground motion has a 2% probability of exceedance within 50 years. Together, the figures depict the lateral load–displacement relationship of the PD-RC control specimen during the pseudodynamic test at  $2 \text{ m/s}^2$ .

**Fig. 11** Lateral response load–displacement relationships for specimens strengthened with the HSF system during pseudodynamic testing at  $2 \text{ m/s}^2$  (first floor)

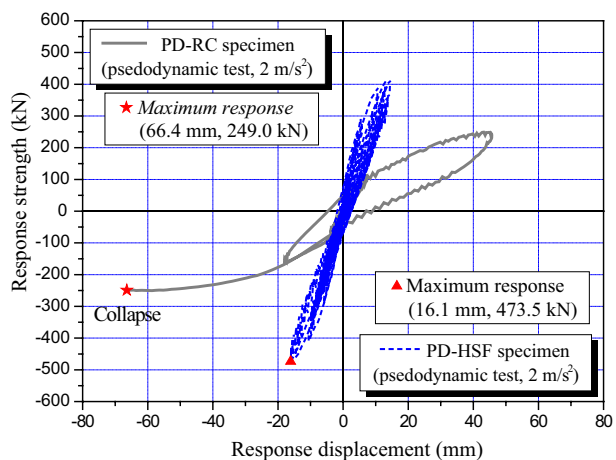




**Fig. 12** Lateral response load–displacement relationships for specimens strengthened with the HSF system during pseudodynamic testing at 3 m/s<sup>2</sup> (first floor)

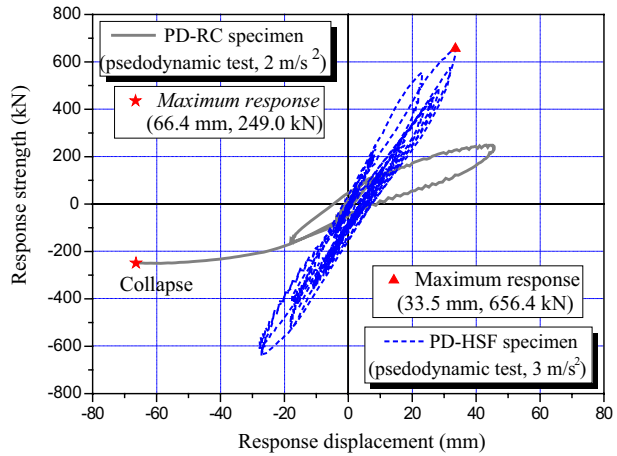


**Fig. 13** Lateral response load–displacement relationships for specimens strengthened with the HSF system during pseudodynamic testing at 4 m/s<sup>2</sup> (first floor)

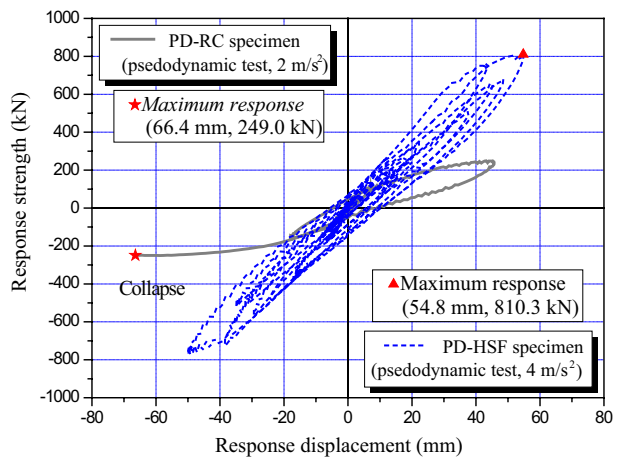


Table 4 presents a comparison of maximum response strength, maximum response displacement, and degree of earthquake damage in the pseudodynamic test for the PD-RC specimen at 2 m/s<sup>2</sup> and for the PD-HSF specimen at 2, 3, and 4 m/s<sup>2</sup> (first floor). The degree of earthquake damage was estimated based on the technique for postearthquake damage evaluation of RC buildings proposed by the JBDPA (2017) and Maeda et al. (2004).

The maximum earthquake response of the PD-RC control specimen for an earthquake ground motion of 2 m/s<sup>2</sup> was observed under a load of 249.0 kN with lateral displacement of 66.4 mm; the target frame finally collapsed at approximately 3.4 s, when the maximum seismic response was observed. The degree of earthquake damage was estimated to be at the collapse level according to JBDPA (2017) and Maeda et al. (2004). However, for an earthquake ground motion of 2 m/s<sup>2</sup> the PD-HSF specimen showed a maximum response strength of 473.5 kN with displacement of 16.1 mm, suffering slight earthquake damage as minor shear cracks, whereas the PD-RC control specimen showed sustained shear collapse. The strength ratio of the reinforced specimen at 2 m/s<sup>2</sup> was 1.9-fold higher than that of the control specimen. At 3 m/s<sup>2</sup>, a maximum response strength of 656.4 kN with lateral

**Table 4** Comparison of response strength, response displacement, and degree of earthquake damage among specimens following pseudodynamic testing (first floor)

Specimen	Input earthquake intensity ( $m/s^2$ )	Maximum response strength and strength ratio* $V_{max}$ (kN)	Response displacement at the maximum point $\Delta_{max}$ (mm)	Failure mode	Degree of earthquake damage**
PD-RC	2	249.0	66.4	Shear failure	Collapse
PD-WERCF	2	473.5 (1.90 = 473.5/249.04)*	16.1	Shear crack	Slight
	3	656.4 (2.64 = 656.37/249.04)*	33.5		Light
	4	810.3 (3.25 = 810.34/249.04)*	54.8		Moderate

\* Strength ratio is the maximum response strength of a specimen strengthened with HSF at each earthquake intensity level relative to that of the control specimen at  $2 m/s^2$ .

\*\* Degree of earthquake damage estimated based on results reported by JBDPA (2017) and Maeda et al. (2004)

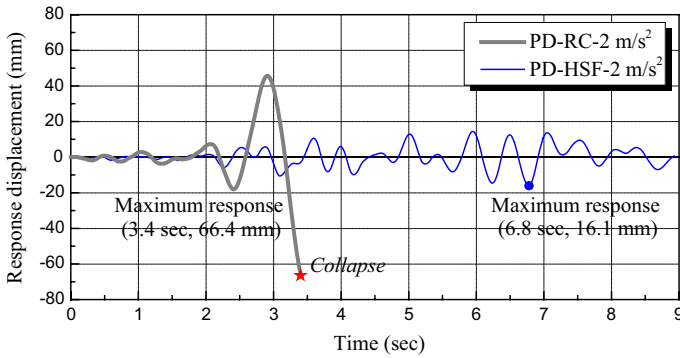


**Fig. 14** Response displacement–time history relationships of the control specimen and HFS- strengthened specimen during pseudodynamic testing at 2 m/s<sup>2</sup> (first floor)

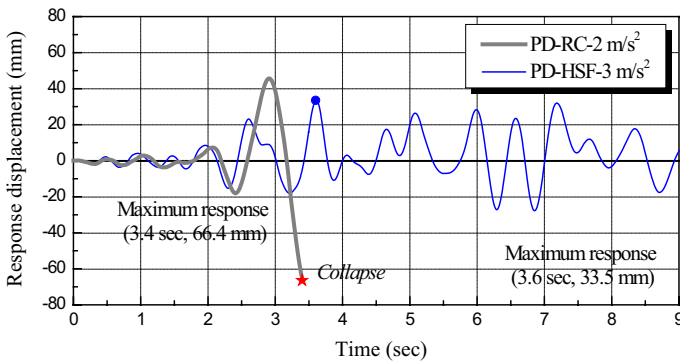


**Fig. 15** Response displacement–time history relationships of the control specimen and HFS- strengthened specimen during pseudodynamic testing at 3 m/s<sup>2</sup> (first floor)

displacement of 33.5 mm was observed, resulting in light earthquake damage. The strength ratio of the HSF specimen at 3 m/s<sup>2</sup> was 2.64-fold higher than that of the control specimen under 2 m/s<sup>2</sup>.

Under severe earthquake ground motion (4 m/s<sup>2</sup>), the PD-HSF specimen showed a maximum earthquake response of 810.34 kN with lateral displacement of 54.79 mm. The strength ratio was 3.25-fold higher than that of the control specimen under 2 m/s<sup>2</sup>. Earthquake damage at 4 m/s<sup>2</sup> was estimated as moderate, according to JBDPA (2017) and Maeda et al. (2004). These results reveal that the HSF methodology is useful for seismic strengthening of building systems, especially in terms of increasing ultimate strength.

### 5.3 Response displacement–time history relationships and maximum displacement

Figures 14, 15, and 16 show response displacement–time history relationships (first floor) of the PD-HSF specimen during pseudodynamic testing at 2, 3, and 4 m/s<sup>2</sup>,

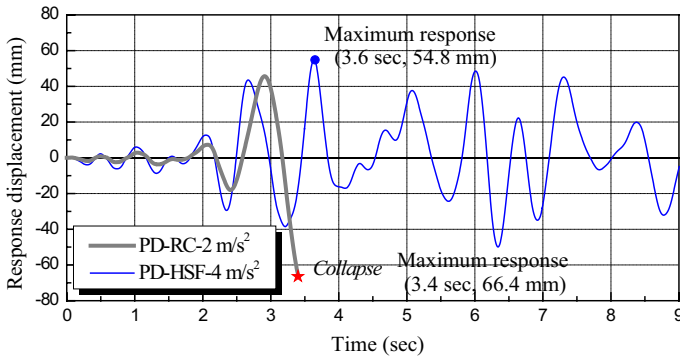


**Fig. 16** Response displacement–time history relationships of the control specimen and HFS- strengthened specimen during pseudodynamic testing at 4 m/s<sup>2</sup> (first floor)

respectively, as well as that of the PD-RC control specimen at 2 m/s<sup>2</sup> EW ground motion recorded at Hachinohe during the 1968 Tokachi-oki earthquake.

At 2 m/s<sup>2</sup>, the maximum response displacement of the PD-RC control specimen occurred at 3.4 s, with a lateral drift of 66.4 mm, resulting in shear collapse of the column. However, the strengthened PD-HSF specimen suffered only slight damage, with a maximum response displacement of 16.1 mm at 6.8 s. At 3 m/s<sup>2</sup>, the PD-HSF specimen showed a maximum response displacement at 3.6 s, with a lateral drift of 33.5 mm, resulting in light damage. At the maximum earthquake intensity (4 m/s<sup>2</sup>), the PD-HSF specimen strengthened with the HSF showed a maximum response displacement of 54.8 mm at 3.6 s and suffered moderate damage including shear cracks.

The earthquake response parameter of primary interest is the decrease in maximum response displacement of the specimens strengthened by the HSF system relative to the control. Table 5 lists these values as percentages, allowing comparison of maximum response displacement between the PD-RC control and PD-HSF-reinforced specimen. The specimen reinforced with the HSF had displacement responses approximately 76% lower than that of the nonstrengthened control specimen at ground acceleration of 2 m/s<sup>2</sup>. At 3 m/s<sup>2</sup>, the PD-HSF specimen showed displacement responses approximately 50% lower than that of the control specimen. At the highest level of earthquake intensity (4 m/s<sup>2</sup>), the strengthened specimen showed displacement responses 18% lower than that of the nonstrengthened control specimen.

**Table 5** Maximum response displacement at 3 m/s<sup>2</sup> and the decrease thereof for test specimens in comparison with the control

Specimen	Input earthquake intensity (m/s <sup>2</sup> )	Maximum response displacement (mm)	Decrease in response displacement of ESRCF-strengthened specimens relative to control (%)
PD-RC	2	66.4	–
PD-HFS	2	16.1	76 (16.1 vs. 66.4 mm)
	3	33.5	50 (33.5 vs. 66.4 mm)
	4	54.8	18 (54.8 vs. 66.4 mm)

## 6 Comparison of nonlinear dynamic analysis and pseudodynamic test results

Based on the results of the pseudodynamic tests presented in Sect. 5, hysteresis models for each member, including beams, columns, strengthening members, and anchor bolts were constructed for nonlinear dynamic analysis. Nonlinear dynamic analysis was conducted based on the proposed hysteresis models and the results were compared with those of the pseudodynamic tests.

### 6.1 Overview of nonlinear dynamic analysis

The specimens used in the nonlinear dynamic analysis were one two-story full-scale unreinforced specimen (PD-RC) and one specimen strengthened using the HSF strengthening method (PD-HSF). Although real structures exhibit complex three-dimensional (3D) vibrations, we replaced the columns, beams, and walls with linear members to model the specimen structure as plane frames considering only the horizontal seismic force, which corresponded to the system used in the pseudodynamic tests.

The characteristics of each floor were evaluated considering the level of each member. The following assumptions were also made: (1) the location of the yield hinge of each member was assumed to be in accordance with JBDPA (2017) and AIJ (2010), and the joint of the column and beam, and the area from the center of each member to the end of the member at which the yield hinge takes place, were assumed to be rigid. (2) The strength capacity of the beam considered the influence of the slab reinforcing bar on the effective width of the slab.

In addition, each member was assumed to resemble the model shown in Fig. 17, with the flexural spring, shear spring, and axial spring serially connected. The control PD-RC specimen also consisted of the walls at the foundation and a grade beam, as shown in Fig. 17a. The control specimen had two floors and 12 nodes including the support point. The PD-HSF-strengthened specimen included an additional reinforcing steel frame and joints in the plane of the existing RC frame, as shown in Fig. 17b. Anchor bolts connecting the existing RC frame and the HSF system were idealized using a link joint element, for a total of 20 nodes.

The nonlinear dynamic analysis was conducted using CANNY, a 3D nonlinear dynamic structural analysis computer program designed by Li (2009). Table 6 shows a summary of the hysteresis models for each member used in the nonlinear dynamic analysis, which are specified in CANNY (Li 2009).

### 6.2 Comparison and analysis of experimental results

The nonlinear dynamic analysis was conducted using CANNY (Li 2009) at the 2 and 3 m/s<sup>2</sup> EW ground motions recorded at Hachinohe during the 1968 Tokachi-oki earthquake. As previously stated, the Hachinohe (EW) ground motion of 2 m/s<sup>2</sup> was applied to the unreinforced control specimen during pseudodynamic testing and the HSF-reinforced specimen applied the Hachinohe (EW) 2–3 m/s<sup>2</sup> motions.

Figure 18 compares the lateral response load–displacement and response displacement–time history relationships between the pseudodynamic test and nonlinear dynamic analysis results for the control specimen (PD-RC) under 2 m/s<sup>2</sup>. Figures 19 and 20 show the lateral response load–displacement and response displacement–time history

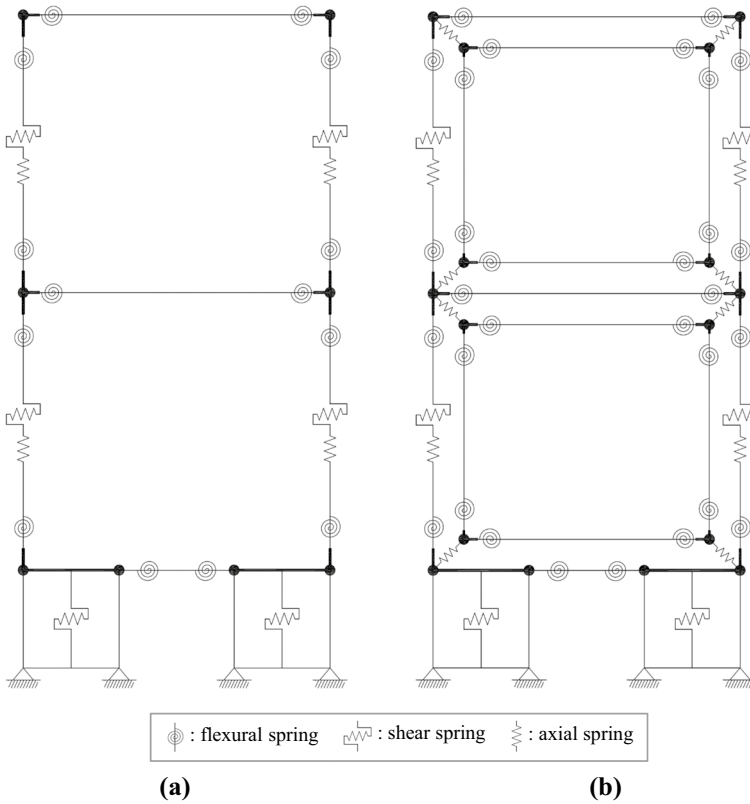


**Fig. 17** Analysis model applied to specimens. **(a)** Control specimen (PD-RC). **(b)** HSF-strengthened specimen (PD-HSF)

**Table 6** Hysteresis models used in the nonlinear dynamic analysis

Members	Hysteresis model	Model description
Beam	Flexural spring	CP3 Cross-peak trilinear model
	Shear spring	OO3 Trilinear origin-oriented
Column	Flexural spring	CA7 CANNY sophisticated trilinear hysteresis model
	Shear spring	OO3 Trilinear origin-oriented
	Axial spring	AE1 Axial stiffness model
Wall	Shear spring	OO3 Trilinear origin-oriented
Anchor bolt	Shear spring	EL2 Bilinear elastic model
Strengthening member (H-beams)	Flexural spring	BL2 Degrading bilinear model
	Shear spring	EL1 Linear elastic model

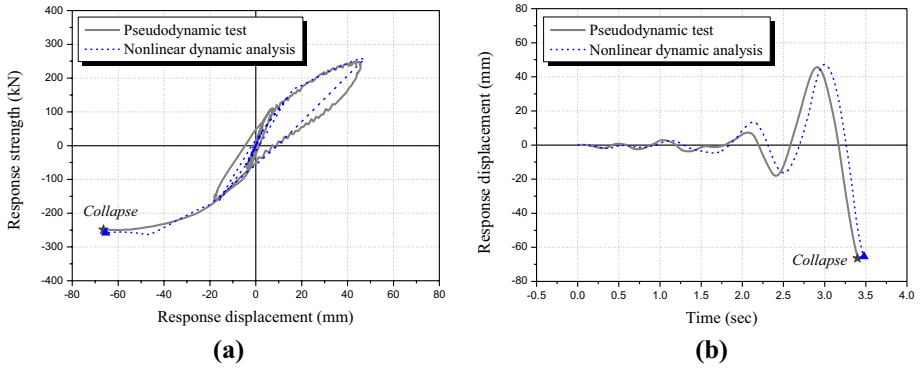


**Fig. 18** Relationships between pseudodynamic test and nonlinear dynamic analysis results for the PD-RC control specimen at  $2\text{ m/s}^2$ . (a) Lateral response load–displacement and (b) displacement–time history

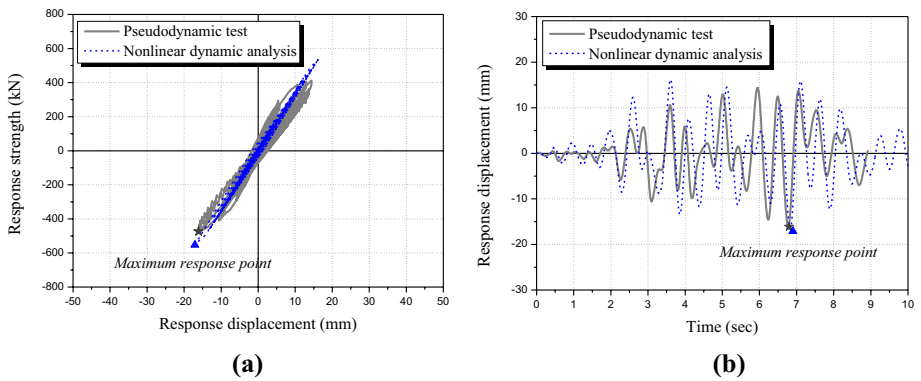


**Fig. 19** Relationships between pseudodynamic test and nonlinear dynamic analysis results for the PD-HSF specimen at  $2\text{ m/s}^2$ . (a) Lateral response load–displacement and (b) displacement–time history

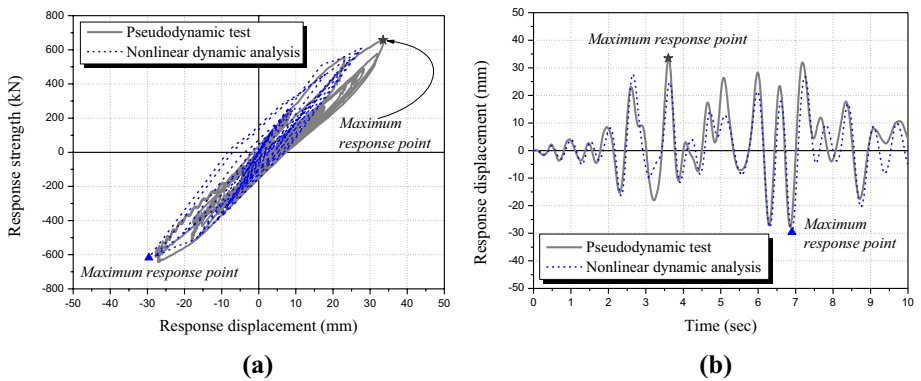


**Fig. 20** Relationships between pseudodynamic test and nonlinear dynamic analysis results for the PD-HSF specimen at  $3\text{ m/s}^2$ . (a) Lateral response load–displacement and (b) displacement–time history

**Table 7** Comparison between specimens of maximum lateral response strength and displacement values

Specimen	Input earthquake intensity ( $m/s^2$ )	Method	Maximum response strength and strength deviation ratio* $V_{max}$ (kN)	Response displacement at the maximum point and displacement deviation ratio $\Delta_{max}$ (mm)
PD-RC	2	Experiment	249.0	66.4
		Analysis	258.0 (1.03)*	65.4 (0.98)*
PD-HSF	2	Experiment	473.5	16.1
		Analysis	552.5 (1.17)*	17.1 (1.06)*
	3	Experiment	656.4	33.5
		Analysis	617.0 (0.94)*	29.6 (0.88)*

\*Deviation ratio indicates values calculated based on maximum response strength (or displacement) of the pseudodynamic test result divided by the nonlinear dynamic analysis result



relationships of the HSF specimen calculated from the nonlinear dynamic analysis at 2 and 3 m/s<sup>2</sup>, respectively, as well as those of the pseudodynamic test. Table 7 lists the maximum response strength and maximum response displacement derived from the results, and compares these to the experimental results.

At an earthquake ground motion of 2 m/s<sup>2</sup>, the control specimen (PD-RC) showed a maximum response strength of 258.0 kN with displacement of 65.4 mm in the dynamic analysis, and the test results showed a strength of 249.0 kN with displacement of 66.4 mm (Fig. 18, Table 7). The HSF-strengthened specimen (PD-HSF) at 2 m/s<sup>2</sup> showed a maximum response strength of 552.5 kN with displacement of 17.1 mm in the dynamic analysis, and the test result showed 473.5 kN and 16.1 mm (Fig. 19, Table 7). For both specimens at 2 m/s<sup>2</sup>, the difference in results between the nonlinear dynamic analysis and pseudodynamic test was within the range of approximately  $\pm 10\%$ , indicating very similar results. At 3 m/s<sup>2</sup>, the HSF-strengthened specimen (PD-HSF; Fig. 20) showed a maximum response strength of 617.0 kN with displacement of 29.6 mm in the dynamic analysis, whereas the test results showed 656.4 kN and 33.5 mm, also indicating a very good result.

These analysis results show that the applied nonlinear analysis models closely simulated the HSF seismic strengthening method and the resulting behavior of the RC frame. It is noteworthy that the seismic reinforcement effects of the HS seismic strengthening methods can be efficiently evaluated using these models and methods.

## 7 Conclusions

In this study, a new HSF system was proposed for seismic strengthening of existing medium-to-low-rise RC buildings to overcome the construction drawbacks of conventional seismic retrofitting techniques. The HSF strengthening method developed in this study exhibits excellent constructability, because a control box is applied as a length adjustment device to cope with errors in the field associated with assembly works between the existing structure and reinforcing frame. This method represents a strength design approach implemented via retrofitting, to easily increase the ultimate lateral load capacity of RC buildings lacking seismic data, which exhibit shear failure. Two full-size two-story RC frame specimens were designed based on an existing RC building in Korea lacking seismic data, and then strengthened using the HSF system; thus, we used one control specimen and one specimen strengthened with the HSF system. Pseudodynamic tests were conducted to verify the effects of seismic retrofitting and earthquake response behavior under the proposed method, in terms of maximum response strength, response displacement, and degree of earthquake damage compared with a control RC frame. We also performed nonlinear dynamic analysis based on the material properties of the test specimens using a mathematical nonlinear hysteresis model, and compared the results to those of the pseudodynamic tests. Test results revealed that the proposed HSF strengthening method installed internally within the RC frame effectively increased its lateral ultimate strength, resulting in reduced response displacement of RC structures under large-scale earthquake conditions. The major results of this work are summarized as follows.

1. The results of the pseudodynamic test on an unreinforced control specimen showed that the specimen experienced shear collapse at a maximum response displacement of 66.4 mm, with lateral strength of 249.0 kN, after approximately 3.4 s under the Hachinohe (EW) input earthquake motion of 2 m/s<sup>2</sup>. Thus, the target RC building is likely vulner-

- able to severe seismic damage in the event of a  $2 \text{ m/s}^2$  earthquake. These results provide important practical data, demonstrating the necessity of applying seismic retrofitting to RC buildings with non-seismic details built in the 1980s.
2. The specimen strengthened by the HSF system exhibited a maximum response strength of 473.5 kN with displacement of 16.1 mm under  $2 \text{ m/s}^2$ , and a strength of 656.4 kN with displacement of 33.5 mm under  $3 \text{ m/s}^2$ . The specimen sustained light earthquake damage under  $2\text{--}3 \text{ m/s}^2$ . Under severe earthquake ground motion of  $4 \text{ m/s}^2$ , the specimen exhibited a maximum response strength of 810.34 kN with displacement of 54.8 mm, and a moderate degree of damage was observed, thereby validating the HSF method.
  3. The earthquake response strength of the HSF-strengthened specimen increased approximately 1.9-fold under input earthquake motion of  $2 \text{ m/s}^2$ , 2.64-fold under  $3 \text{ m/s}^2$ , and 3.25-fold under  $4 \text{ m/s}^2$ , compared to the unreinforced control specimen. Compared to the control specimen, response displacement was suppressed in the HSF-strengthened specimen by approximately 76% at  $2 \text{ m/s}^2$ , by 50% at  $3 \text{ m/s}^2$ , and by 18% at  $4 \text{ m/s}^2$ .
  4. Based on the results of the pseudodynamic tests, hysteresis models for each member, including beams, columns, strengthening members, and anchor bolts were constructed for the nonlinear dynamic analysis. Nonlinear dynamic analysis was conducted based on these hysteresis models and the results were compared with those of pseudodynamic tests. The applied nonlinear analysis models closely simulated the HSF seismic strengthening methods and the behavior of the resulting RC frame. The seismic reinforcement effects of the HS seismic strengthening methods can therefore be efficiently evaluated using these applied models and methods.
  5. These test and analysis results demonstrate that the HSF method proposed in this study for existing medium-to-low-rise RC buildings lacking seismic data effectively increased the lateral ultimate strength of the structures, resulting in a reduction in response displacement under large-scale, intense earthquake conditions. The HSF system exhibits excellent constructability because a control box is applied as a length adjustment device to cope with any errors that may occur in the field in association with assembly works to connect the existing structure and reinforcing frame. The new method also increases the ultimate lateral load capacity of existing RC buildings with shear failure mode.
  6. The HSF strengthening method appears to be a suitable candidate for commercialization. Future studies should aim to develop guidelines for conducting seismic strengthening procedures including the amount of reinforcement required for practical purposes. Seismic performance before and after strengthening should also be compared through nonlinear dynamic analysis of an entire RC building strengthened by the HSF system.

**Acknowledgements** This research was supported by the Korea Agency for Infrastructure Technology Advancement Grant (20CTAP-C153033-02) from the Ministry of Land, Infrastructure, and Transport Affairs of the Korean government.

**Data availability** All datasets generated in this study are available from the corresponding author upon reasonable request.

## Compliance with ethical standards

**Conflict of interest** The authors declare no competing interests.

## References

- ACI (American Concrete Institute) (2014) 318–14: Building code requirements for structural concrete and commentary. ACI, MI, USA
- AIJ (Architectural Institute of Japan) (1968) Report on damage due to the 1968 Tokachi-oki earthquake. Tokyo, Japan (in Japanese)
- AIJ (Architectural Institute of Japan) (2010) Standard for structural calculation of reinforced concrete structures. AIJ, Tokyo, Japan (in Japanese)
- Abou-Elfath H, Ghobarah A (2000) Behavior of reinforced concrete frames rehabilitated with concentric steel bracing. *Can J Civ Eng* 27:433–444
- Ariyaratana C, Fahnestock LA (2011) Evaluation of buckling-restrained braced frame seismic performance considering reserve strength. *Eng Struct* 33:77–89
- Badoux M, Jirsa O (1990) Steel bracing of RC frames for seismic retrofitting. *J Struct Eng ASCE* 116(1):55–74
- Bursi OS, Shing PB, Radakovic-Guzina Z (1994) Pseudodynamic testing of strain-softening systems with adaptive time steps. *Earthq Eng Struct Dyn* 23(7):745–760
- Bursi OS, Shing PB (1998) Evaluation of some implicit time-stepping algorithms for pseudodynamic tests. *Earthq Eng Struct Dyn* 25(4):333–355
- Celik OC, Bruneau M (2009) Seismic behavior of bidirectional-resistant ductile end diaphragms with buckling restrained braces in straight steel bridges. *Eng Struct* 31:380–393
- FEMA (Federal Emergency Management Agency) (1998) FEMA 310: Handbook for seismic evaluation of buildings—a prestandard. FEMA, Washington, DC, USA
- FEMA (Federal Emergency Management Agency) (2000) FEMA 356: Prestandard and commentary for seismic rehabilitation of buildings. FEMA, Washington, DC, USA
- Ghobarah A, Abou-Elfath H (2001) Rehabilitation of a reinforced concrete frames using eccentric steel bracing. *Eng Struct* 23:745–755
- Hilber HM, Hughes TJ, Taylor RL (1977) Improved numerical dissipation for time integration algorithms in structural dynamics. *Earthq Eng Struct Dyn* 5(3):283–292
- Hwang JS, Lee KS (2016) Seismic strengthening effects based on pseudodynamic testing of a reinforced concrete building retrofitted with a wire-woven bulk kagome truss damper. *Shock Vib* 2016(3956126):17
- IBC (International Building Code) (2018) 2018 International building code. The International Code Council, USA
- JBDPA (Japan Building Disaster Prevention Association) (2017) Standard for damage level classification. JBDPA, Tokyo, Japan
- JBDPA (Japan Building Disaster Prevention Association) (2005) Standard for seismic evaluation of existing reinforced concrete buildings, guidelines for seismic retrofit of existing reinforced concrete buildings, and technical manual for seismic evaluation and seismic retrofit of existing reinforced concrete buildings. JBDPA, Tokyo, Japan
- Ju M, Lee KS, Sim J, Kwon H (2014) Non-compression cross-bracing system using carbon fiber anchors for seismic strengthening of RC structures. *Mag Concr Res* 66(4):159–174
- KBC (Korean Building Code) (2016) 2016 Korean building code. Architectural Institute of Korea, Seoul, Korea (in Korean)
- KS B 0801(2017) Test pieces for tension test for metallic materials. Korean Industrial Standards, Korea (in Korean)
- Kunisue A, Koshika N, Kurokawa Y, Suzuki N, Agami J, Sakamoto M (2000) Retrofitting method of existing reinforced concrete buildings using elasto-plastic steel dampers. In: Proceedings of 12th world conference on earthquake engineering, Auckland, New Zeland
- Lee KS (2010) Seismic capacity requirements for low-rise reinforced concrete buildings controlled by both shear and flexure. *J Adv Concr Technol* 8(1):75–91
- Lee KS (2015) An experimental study on non-compression X-bracing systems using carbon fiber cable for seismic strengthening of RC buildings. *Polymers* 7(9):1716–1731
- Lee KS, Nakano Y, Kumazawa H, Okada T (1995) Seismic capacity of reinforced concrete buildings damaged by the 1995 Hyogo-ken Nambu earthquake. *Bulletin of Earthquake Resistant Structure Research Center*, No. 28, Institute of Industrial Science, University of Tokyo, Japan
- Lee KS, Shin SW (2013) A new methodology for performance-based seismic evaluation of low-rise reinforced concrete buildings using nonlinear required strengths. *J Adv Concr Technol* 11:151–166
- Lee KS, Wi JD, Kim YI, Lee HH (1980s) Seismic safety evaluation of Korean R/C school buildings built in the 1980s. *J Korean Inst Struct Maint Insp* 13(5):1–11 (in Korean)

- Li KN (2009) Canny: a 3-dimensional nonlinear dynamic structural analysis computer program, user manual. CANNY Structural Analysis, Vancouver, Canada
- Maeda M, Nakano Y, Lee KS (2004) Postearthquake damage evaluation for RC buildings based on residual seismic capacity. In: Proceedings of 13th world conference on earthquake engineering, No. 1179, Vancouver, Canada
- Maheri MR, Kousari R, Razazan M (2003) Pushover tests on steel X-braced and knee-braced RC frames. *Eng Struct* 25:1697–1705
- Mahin SA, Shing PB (1985) Pseudodynamic method for seismic testing. *J Struct Eng* 111(7):1482–1503
- Marko J, Thambiratnam D, Perera N (2004) Influence of damping systems on building structures subject to seismic effects. *Eng Struct* 26(13):1939–1956
- MTS (2002) Pseudodynamic testing for 793 controllers. MTS Systems Corporation, Eden Prairie, MI, USA
- Nateghi-Alahi F (1995) Seismic strengthening of eight-storey RC apartment building using steel braces. *Eng Struct* 17(6):455–461
- Oliveto G, Caliò I, Marletta M (2004) Retrofitting of Reinforced Concrete Buildings Not Designed to Withstand Seismic Action: A Case Study Using Base Isolation. In: Proceedings of the 13th world conference on earthquake engineering, Vancouver, Canada, Paper No. 954
- Onat O, Correia AA, Lourenço PB, Koçak A (2018) Assessment of the combined in-plane and out-of-plane behavior of brick infill walls within reinforced concrete frames under seismic loading. *Earthq Eng Struct Dyn* 47:2821–2839
- Sarno L, Elnashai AS (2009) Bracing systems for seismic retrofitting of steel frames. *J Constr Steel Res* 65:452–465
- Shing PB, Mahin SA, Dermitzakis SN (1984) Evaluation of on-line computer control methods for seismic performance testing. In: Proceedings of 8th world conference on earthquake engineering, San Francisco, CA
- Shing PB, Mahin SA (1985) Computational aspects of a seismic performance test method using on-line computation control. *Earthq Eng Struct Dyn* 13:507–526
- Shing PB, Nakashima M, Bursi OS (1996) Application of pseudodynamic test method to structural research. *Earthq Spectra* 12(1):29–56
- Smith ST, Kim SJ (2008) Shear strength and behavior of FRP spike anchors in FRP-to-concrete joint assemblies. In: Proceedings of fifth international conference on advanced composite materials in bridges and structures (ACMBS-V), ISBN. 978-0-9736430-7-7
- SSRG (Seismic Strengthening Research Group) (2008) Seismic strengthening of RC buildings. Ohmsha Press, Tokyo, Japan (in Japanese), SSRG
- Sugano S (1981) Seismic strengthening of existing reinforced concrete buildings in Japan. *Bull N Z Natl Soc Earthq Eng* 14(4):209–222
- Suzuki N, Koshika N, Kurokawa Y, Yamada T, Takahashi M, Tagami J (1998) Retrofitting method of existing reinforced concrete buildings using elasto-plastic steel damper. In: Second world conference on structural control, Kyoto, Japan, pp 227–234
- Takanashi K, Udagawa K, Tanaka H (1980) Pseudo-dynamic tests on a 2-storey steel frame by a computer-load test apparatus hybrid system. In: Proceedings of the 7th world conference on earthquake engineering, 7: 225–232, Istanbul, Turkey
- Tokyo Soki Kenkyujo Company (2020) Tokyo, Japan. <https://www.tml.jp/e/>
- Witt S (2007) Development in fiber roving anchors for use with externally bonded fiber reinforced polymers. In: Proceedings of 8th international symposium on fiber reinforced polymer reinforcement for concrete structures, paper No. 15–11